

Original Article

Tumor shrinkage by cyclopamine tartrate through inhibiting hedgehog signaling

Qipeng Fan^{1*}, Dongsheng Gu^{1*}, Miao He^{1,2*}, Hailan Liu^{1*}, Tao Sheng¹, Guorui Xie¹, Ching-xin Li³, Xiaoli Zhang¹, Brandon Wainwright⁴, Arash Garrossian⁵, Massoud Garrossian⁵, Dale Gardner⁶ and Jingwu Xie¹

Abstract

The link of hedgehog (Hh) signaling activation to human cancer and synthesis of a variety of Hh signaling inhibitors raise great expectation that inhibiting Hh signaling may be effective in human cancer treatment. Cyclopamine (Cyc), an alkaloid from the *Veratrum* plant, is a specific natural product inhibitor of the Hh pathway that acts by targeting smoothened (SMO) protein. However, its poor solubility, acid sensitivity, and weak potency relative to other Hh antagonists prevent the clinical development of Cyc as a therapeutic agent. Here, we report properties of cyclopamine tartrate salt (CycT) and its activities in Hh signaling-mediated cancer *in vitro* and *in vivo*. Unlike Cyc, CycT is water soluble (5–10 mg/mL). The median lethal dose (LD₅₀) of CycT was 62.5 mg/kg body weight compared to 43.5 mg/kg for Cyc, and the plasma half-life (T_{1/2}) of CycT was not significantly different from that of Cyc. We showed that CycT had a higher inhibitory activity for Hh signaling-dependent motor neuron differentiation than did Cyc (IC₅₀ = 50 nmol/L for CycT vs. 300 nmol/L for Cyc). We also tested the antitumor effectiveness of these Hh inhibitors using two mouse models of basal cell carcinomas (K14cre:*Ptch*^{1^{neo/neo}} and K14cre:*Smo*M2^{YFP}). After topical application of CycT or Cyc daily for 21 days, we found that all CycT-treated mice had tumor shrinkage and decreased expression of Hh target genes. Taken together, we found that CycT is an effective inhibitor of Hh signaling-mediated carcinogenesis.

Key words Cyclopamine tartrate, hedgehog, smoothened, cancer therapy, mouse model

The hedgehog (Hh) pathway plays an important role in embryonic development, tissue polarity, cell

proliferation, and carcinogenesis^[1-5]. Smoothened (SMO), the seven transmembrane domain-containing protein, serves as the key player for signal transduction of this pathway, whose function is inhibited by patched (PTC), another transmembrane protein, in the absence of Hh ligands^[6,7]. Binding Hh to its receptor PTC releases this inhibition, allowing SMO to signal downstream, eventually to Gli transcription factors. As transcription factors, Gli molecules can regulate target gene expression by direct association with a specific consensus sequence located in the promoter region of target genes^[8,9]. Hh signaling has been reported to be activated in many types of human cancer, including cancers of the skin, brain, gastrointestinal tract, prostate, lung, and breast^[6,10-14]. Thus, the discovery and synthesis of specific signaling antagonists for the Hh pathway has significant clinical implications in novel cancer

Author's Affiliations: ¹Wells Center for Pediatric Research, Department of Pediatrics and The Simon Cancer Center, Indiana University, Indianapolis, IN 46202, USA; ²Key Laboratory for Oral Biomedical Engineering of Ministry of Education, School and Hospital of Stomatology, Wuhan University, Wuhan, Hubei 430079, P. R. China; ³Department of Dermatology Xijing Hospital, Xi'an, Shaanxi 710032, P.R. China; ⁴Institute for Molecular Bioscience, The University of Queensland, Brisbane, QLD 4072, Australia; ⁵Logan Natural Products Inc., Dallas, TX 75025, USA; ⁶United States Department of Agriculture, Agriculture Research Services, Poisonous Plant Research Laboratory, Logan, UT 84341, USA.

Corresponding Author: Jingwu Xie, Wells Center for Pediatric Research, Department of Pediatrics and The Simon Cancer Center, Indiana University, 980 W. Walnut St., Indianapolis, IN 46202. Tel: +1-317-278-3999; Fax: +1-317-274-8046. Email: jinxie@iupui.edu.

*The first four authors contributed equally to this work.

doi: 10.5732/cjc.011.10157

therapeutics^[15]. Cyclopamine (Cyc), a plant alkaloid, was the first described Hh signaling inhibitor^[16,17]. However, the poor solubility and the low potency of Cyc prevent its clinical usage.

To increase the solubility and efficacy of Cyc, we generated cyclopamine tartrate (CycT) through reaction of Cyc with tartaric acid. Here, we report the properties of CycT and its effectiveness in inhibiting hedgehog signaling-mediated carcinogenesis.

Materials and Methods

Mice

Krt14-cre mice^[18], obtained from the eMICE NCI Mouse Repository program, R26-*SmoM2^{YFP}* mice^[19], purchased from the Jackson Laboratory (Bar Harbor, ME, USA), and Krt6a-cre:*Ptch1^{neo/neo}* mice, which were generated as described previously^[20], were maintained and mated under pathogen-free husbandry conditions. The offspring was screened using PCR to determine their transgenic status according to the instruction from the vendors. All animal studies were approved by Institutional Animal Care and Use Committee at Indiana University.

Hh inhibitors

Cyc was isolated and purified as previously described^[21]. 3-Keto-N-(aminoethyl-aminocaproyl-dihydrocinnamoyl) (KAAD)-Cyc^[17] was purchased from Toronto Natural Products, Inc. (Toronto, ON M5R 2G3, Canada).

CycT (Figure 1) was generated by reacting 1 mole of tartaric acid with 2 moles of Cyc. The mixture was heated until the solution volume decreased to one third, after which diethyl ether was added. The solution was then cooled, filtered, and precipitated. The purity of CycT was examined by high-pressure liquid chromatography.

Assessment of acute toxicity

The acute toxicity and LD₅₀ of Cyc and CycT were evaluated using 129S1/SvImJ mice, weighing 18 to 22 g (stock number 002448, Jackson Laboratory, Bar Harbor, ME, USA). Cyc and CycT were dissolved in 100% ethanol, diluted in saline buffer to a final concentration of 5% ethanol, and intraperitoneally administered to mice at different doses, with 10 mice per dose. An additional 10 mice were treated with the same volume of 5% ethanol in saline buffer (control). The end-point was death or survival 7 days after treatment.

Analysis of Cyc and CycT in mouse blood samples

After Cyc or CycT administration, blood was drawn from the mouse tail vein at different time points (0, 0.5, 1, 3, 4, 8, 16, 24, 28 h) and kept at -20°C. For analysis, samples were thawed at room temperature and centrifuged at 12 000 rpm for 5 min in a Beckman benchtop centrifuge. Centrifuged samples were mixed with an equal volume of acetonitrile (Sigma, St. Louis, MO, USA), vortexed for 30 s, and then centrifuged again, as above. The transparent liquid was removed

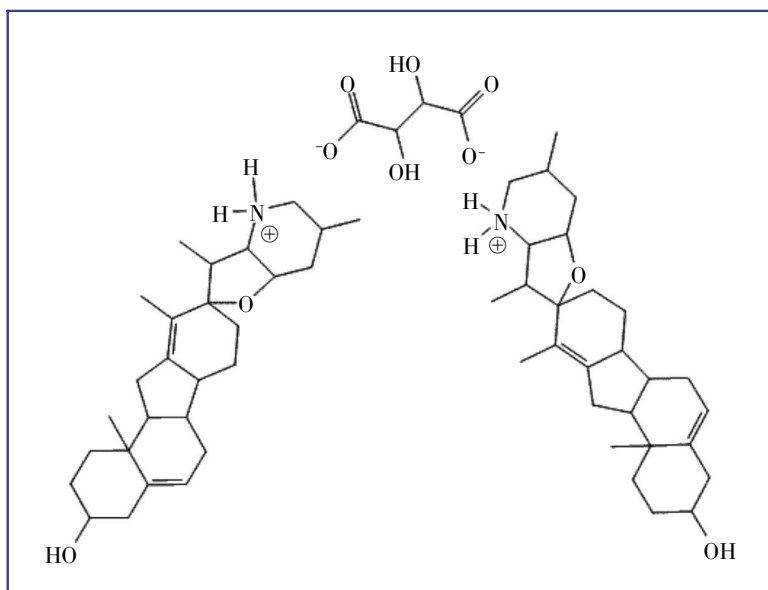


Figure 1. A diagram of the cyclopamine tartrate (CycT) salt structure.

and placed into a micro autosample vial and again centrifuged as above. Samples were then analyzed for Cyc and CycT by liquid chromatography-mass spectrometry using a Thermo Fisher LCQ mass spectrometer equipped with a Surveyor autosampler, MS solvent pump, electrospray ionization source, and Betasil C18 (5 μ , 100 mm \times 2.1 mm) column (Thermo Fisher, Waltham, MA 02454, USA). Samples were eluted with 0.1% formic acid and acetonitrile at a flow rate of 0.300 mL/min as follows: 20% acetonitrile (0–1 min), linear gradient increase from 20% to 60% acetonitrile (1–2 min), isocratic flow of 60% acetonitrile (2–10 min), and returned to 20% acetonitrile (10–11 min), followed by column re-equilibration for 5 min before the next injection. The mass spectrometer was operated in the MS/MS mode scanning a parent ion range of (412.3 \pm 1) *m/z*. Instrument parameters (collision, activation Q, and activation time) were adjusted manually to provide a full scan MS/MS spectrum (100–500 *m/z*) with a parent ion (MH^+ = 412) relative intensity of ~10%. Peak area was measured from reconstructed ion chromatograms generated from the sum of three selected MS/MS ions (321, 377, and 394 *m/z*). Quantitation was based on a 5-point calibration curve (1000, 500, 250, 125, and 31 ng/ μ L) prepared by dilution of a stock solution (1.0 mg/mL Cyc or CycT in 50% acetonitrile) as follows: 20 μ L in 0.980 mL, then 100 μ L in 1.900 mL, followed by serial dilution.

Drug treatment protocol

Mice with basal cell carcinomas were treated with the chemicals daily for 21 days by topical application. Cyc (5 μ mol/L), CycT (0.5 and 5 μ mol/L), and the known Cyc derivative KAAD-Cyc (1 μ mol/L)^[17] were diluted to working concentrations (as indicated) in 70% ethanol and embrocated on the skin surface in the upper and lower areas of the abdomen daily for 21 days. As a control, 70% ethanol was embrocated in the middle belly. Each group had at least 6 mice (6 mice for *Krt6a-cre:Ptch1^{neo/neo}* and 10 mice for *Krt14-cre:SmoM2^{YFP}*) depending the availability of the genotype. At the end of the study, skin biopsies were collected for hematoxylin and eosin (HE) staining. Five sections were obtained from each mouse, and 5 to 8 fields were selected from each section for ImageJ analyses to obtain the percentage of tumor area per field. An average value and standard deviation for all 5 sections was calculated from the values derived from ImageJ for each group. The values from different groups were compared.

Histology and microscopic basal cell carcinoma (BCC) analysis

Skin tissues were collected after each experiment.

Half of the tissue was frozen on dry ice and immediately stored at -80°C . The other half was fixed in 10% formaldehyde overnight, paraffin embedded, sectioned at 5 μ m, and stained with HE. Four to eight epidermal fields were randomly chosen in each section. The viable tumor areas in selected tissue fields were quantified by manually demarcating the tumor boundary on an electronic image of an HE-stained section. The proportion of tumor area to the total tissue field was quantified using ImageJ with 5 fields analyzed for each section (at least 6 mice per group).

RT-PCR and real-time PCR

Total RNA was isolated from the tissues stored at -80°C using TRIzol reagent (Sigma, St. Louis, MO, USA) according to the manufacturers' instructions. One μ g of total RNA was reversely transcribed into cDNA using the first-strand synthesis kit (Roche Applied Science, Indianapolis, IN, USA). Quantitative PCR analyses were performed according to a previously published procedure using primers and probes from Applied Biosystems^[22,23]. Triplicate CT values were analyzed in Microsoft Excel using the comparative CT method as described by the manufacturer (Applied Biosystems, Foster City, CA, USA). The amount of target was obtained by normalization to an endogenous reference (18S RNA) and relative to a calibrator.

Motor neuron differentiation from mouse embryonic stem cells

Mouse embryonic cell line E14Tg2a.4 was purchased from Mutant Mouse Regional Resource Centers at UC Davis (Davis, CA, USA) and cultured according to a procedure from the source (http://www.mmrrc.org/strains/E14/Ctr_protocol.pdf). Motor neuron differentiation was performed according to a previously published protocol^[23]. In short, embryonic bodies were formed from embryonic stem cells (5×10^5 cells/mL) cultured in embryonic stem cell medium without leukemia inhibitory factor (LIF) on ultra-low adhesive plates for 2 days. Motor neurons were induced by addition of retinoic acids (100 nmol/L) and purmorphamine (2.5 μ mol/L) for 5 to 7 days^[24,25]. The effects of CycT, Cyc, KAAD-Cyc on motor neuron differentiation were tested by incubating the compound separately with motor neuron induction medium at given concentrations. Staining for the Hb9 homeobox transcription factor was performed using antibodies from the Development Hybridoma Bank according to manufacturer's instructions.

Statistical analysis

Values of LD_{50} and plasma half-life ($T_{1/2}$) of CycT and Cyc were calculated with the GraphPad Prism software. The results were compared using unpaired Student's *t*-test, with *P* values of < 0.05 indicating statistically significant difference. Power analysis for animal studies was performed with the Statistical Power Calculator from DSS Research (<http://www.dssresearch.com/toolkit/spcalc/power.asp>). With 6 to 10 mice per group, the power of the study was 90 or higher, with a confidence interval of 90%.

Results

Assessment of properties of CycT and Cyc

Solubility of CycT and Cyc was examined by

dissolving them in deionized water at different concentrations. CycT could be dissolved in water at 5-10 mg/mL, whereas Cyc was water insoluble. The formation of the Cyc tartrate salt is predicted to alter Cyc conformation, which may result in changes in bioavailability, biological efficacy, etc. As shown in Figure 2, CycT exhibited a lower acute toxicity ($LD_{50} = 62.5$ mg/kg body weight for CycT vs. 43.5 mg/kg body weight for Cyc). Even considering the molecular weight of tartaric acid (150 Da), the difference between Cyc (411 Da) and CycT was still statistically significant ($P < 0.05$), suggesting that mice are more tolerable to CycT. The plasma $T_{1/2}$ for CycT and Cyc varies from animal to animal, which prevented us to accurately differentiate the two. The plasma $T_{1/2}$ of CycT ranges from 1 to 7.8 h, whereas that of Cyc varies from 1 to 4 h (Figure 2 shows the average value from one experiment with more than 6 mice at each time point).

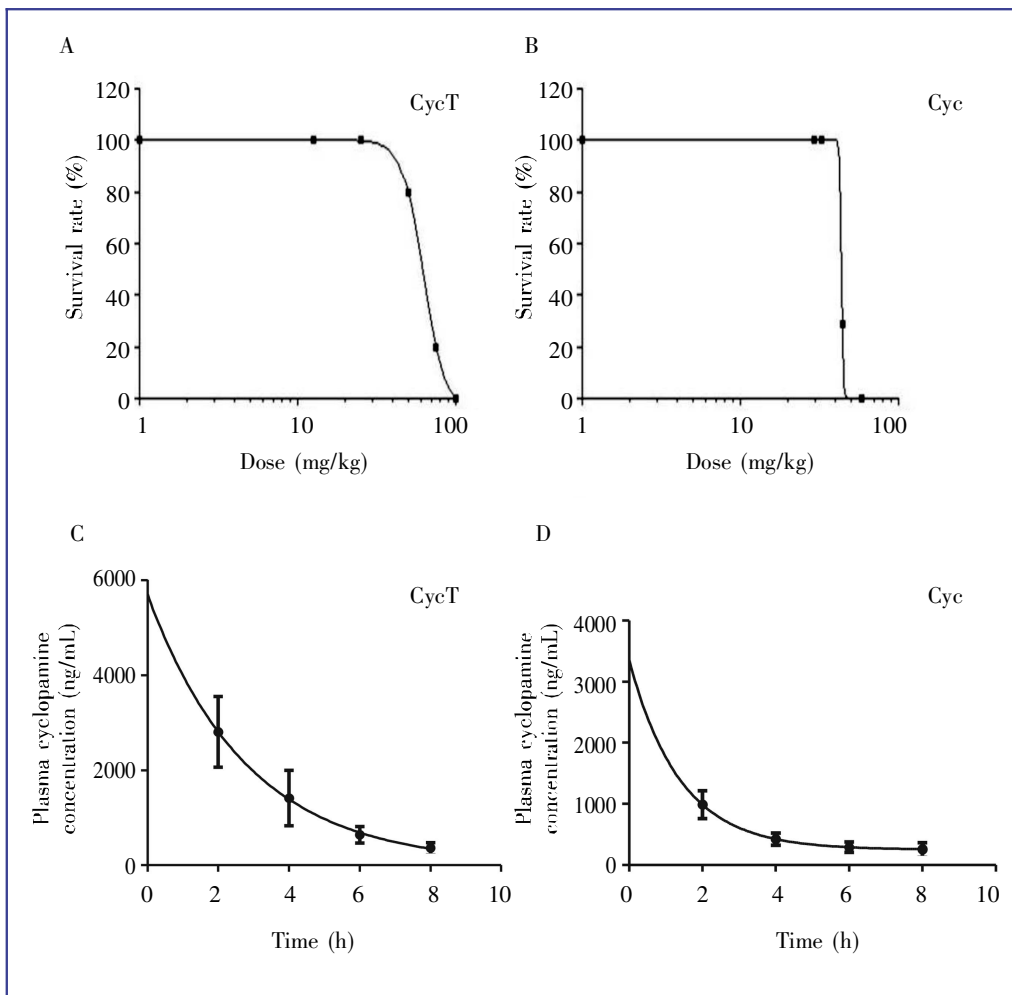


Figure 2. The median lethal dose (LD_{50}) and plasma half-life ($T_{1/2}$) of CycT and cyclopamine (Cyc). The LD_{50} of CycT (A) and Cyc (B) were determined by GraphPad Prism analyses after obtaining the survival data on 129S1/SvlmJ mice injected with different amounts of CycT or Cyc. Unpaired Student's *t*-test showed that the LD_{50} of CycT was significantly higher than that of Cyc (62.5 vs. 43.5 mg/kg body weight, $P < 0.05$). The plasma $T_{1/2}$ values were calculated with GraphPad Prism using the values of plasma CycT (C) or Cyc (D) at different time points following intraperitoneal injection of the compounds into 3-week old mice (6 mice/dose). We observed significant variations of $T_{1/2}$ from mouse to mouse. Figure 2C and 2D showed the average value from one set of experiments. On average, the $T_{1/2}$ of CycT was slightly longer than that of Cyc (1.95 h vs. 0.97 h).

Effects of CycT on motor neuron differentiation

SMO antagonist Cyc and its derivatives are known to suppress the effects of SMO agonists on Hh signaling [17,23], and these antagonistic effects have been widely used to assess drug potency. We used motor neuron differentiation as an Hh signaling readout to test the effectiveness of CycT because the motor neuron differentiation process is Hh signaling-dependent. Motor neuron differentiation was carried out by addition of retinoic acid and SHH (or SMO agonist purmorphamine) to the embryonic bodies derived from ES14Tg2a cells (Figure 3). Purmorphamine was more effective than SHH in this assay [26]. CycT at 50 nmol/L was sufficient to inhibit motor neuron differentiation, with potency similar to KAAD-Cyc. In contrast, Cyc at the same concentration had no significant effects on the expression of motor neuron differentiation markers (data not shown). These

data indicate that CycT is more potent than Cyc in inhibiting Hh signaling-dependent processes.

The effect of CycT on tumors in *Krt6a-cre: Ptch1^{neo/neo}* mice

To examine if CycT is effective *in vivo* in reducing Hh signaling-mediated carcinogenesis, we used *Krt6a-cre:Ptch1^{neo/neo}* mice. As reported previously [20], at 4 months after treatment with retinoic acid, *Krt6a-cre:Ptch1^{neo/neo}* mice developed skin lesions all over the body and the Hh target genes *Gli1*, *Ptch1*, and *Hip* were up-regulated. We performed topical application of CycT, Cyc, and the solvent control (70% ethanol) daily for 21 days. At the end of the study, we determined the tumor areas of treated skin by quantitatively analyzing HE-stained sections.

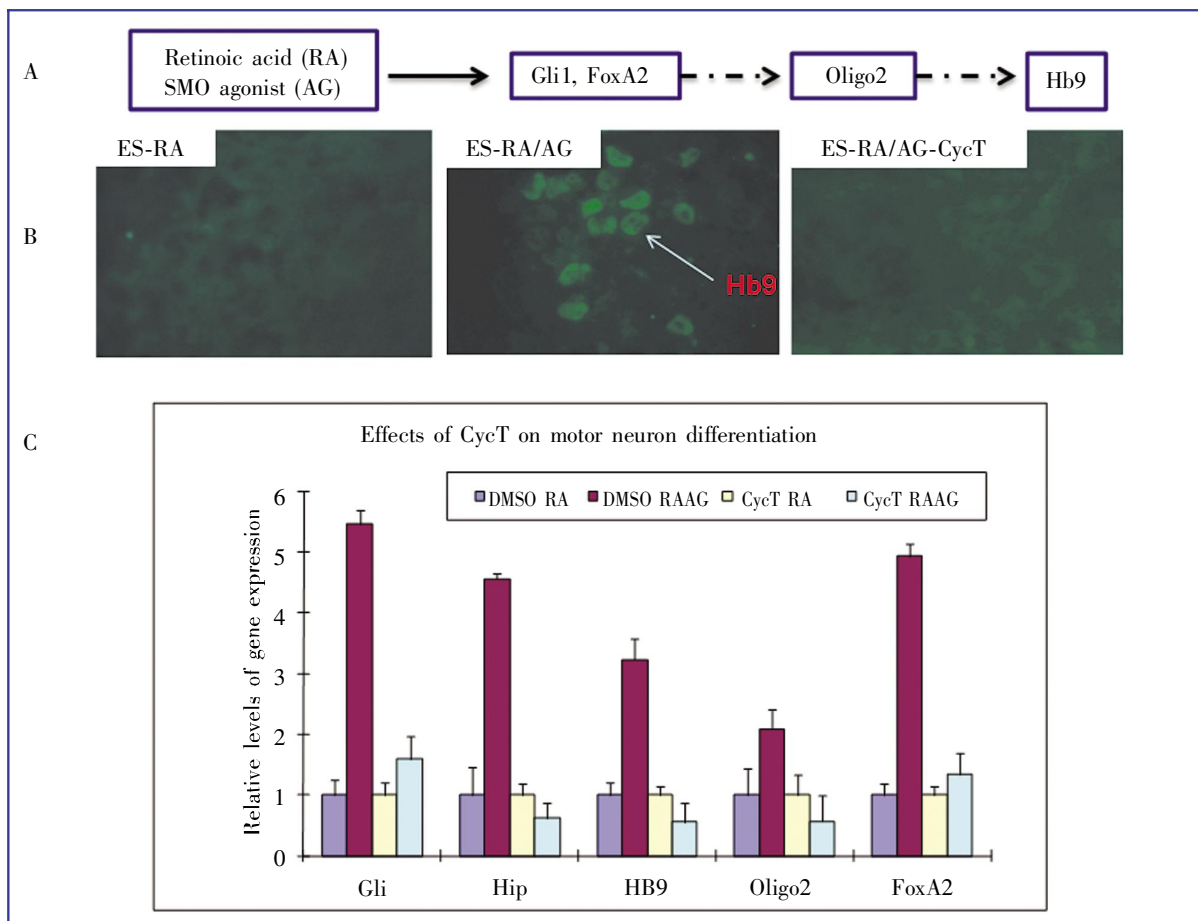


Figure 3. Effect of CycT on motor neuron differentiation. A, the process of motor neuron differentiation. Embryonic stem cells in embryonic bodies can be induced by retinoic acid (RA) and SMO agonist purmorphamine (AG) to express Hh target genes *Gli1* and *FoxA2* as well as expression of motor neuron differentiation markers *oligo2* and *Hb9*. The whole process takes about 5 days. B, immunofluorescent staining with *Hb9* antibody in embryonic bodies of the ES14Tg2a mouse embryonic stem cell line. *Hb9* expression was induced by incubation with RA and AG and inhibited by CycT. C, real-time PCR data on motor neuron differentiation. Expression of Hh target genes *Hip*, *Gli1*, and *FoxA2*, as well as neuron markers *Oligo2* and *Hb9* were examined. In the presence of CycT, no induction of Hh target genes or motor neuron markers was observed.

As shown in Figure 4, CycT at 5 $\mu\text{mol/L}$ reduced tumor area by 60%. Even at a lower concentration (0.5 $\mu\text{mol/L}$), CycT was shown to reduce tumor areas by half. In contrast, the maximum reduction in tumor area in the Cyc treatment group was less than 5% (Figure 5). Notably, mice treated with CycT or control solvent did not exhibit any significant differences in animal behavior, body weight, or lifespan, suggesting that topical application of CycT is not toxic. Taken together, our data in *Krt6a-cre:Ptch1^{neo/neo}* mice indicates that CycT is an effective and non-toxic inhibitor for Hh signaling-mediated tumorigenesis when being applied topically.

Since CycT is an Hh signaling inhibitor, we examined the effect of CycT on Hh target gene expression by real-time PCR analysis. As shown in Figure 4D, we found that CycT decreased expression of Hh target genes *Hip* and *Gli1*. Based on these results, we concluded that CycT decreased tumor areas through inhibiting Hh signaling.

The effect of CycT on tumors in *Krt14-cre:Smom2^{YFP}* mice

In addition, we tested the effect of CycT on tumors in *Krt14-cre:Smom2^{YFP}* mice. As mutant SMO is known to be more resistant to SMO antagonists, we predicted that only potent compounds could inhibit *Smom2^{YFP}*-mediated tumors. By mating *Krt14-cre* mice with *R26-Smom2^{YFP}* mice, we generated *Krt14-cre/R26-Smom2^{YFP}* mice, which have microscopic BCCs all over the body in 8-week old mice [27]. We observed that Hh target genes *Gli1* and *Ptch1* were up-regulated in the skin [27]. These mice were treated with CycT by topical application daily for 21 days, and the tumor area in the skin of the CycT-treated group was compared with that of the control group. We found that CycT significantly reduced tumor area by nearly 30% in the tissue in all mice ($n = 6$) in comparison with the control group (Figures 6A and 6B). The levels of Hh target genes *Gli1* and *Ptch1* in the skin from CycT-treated mice decreased (Figure 6C), indicating the

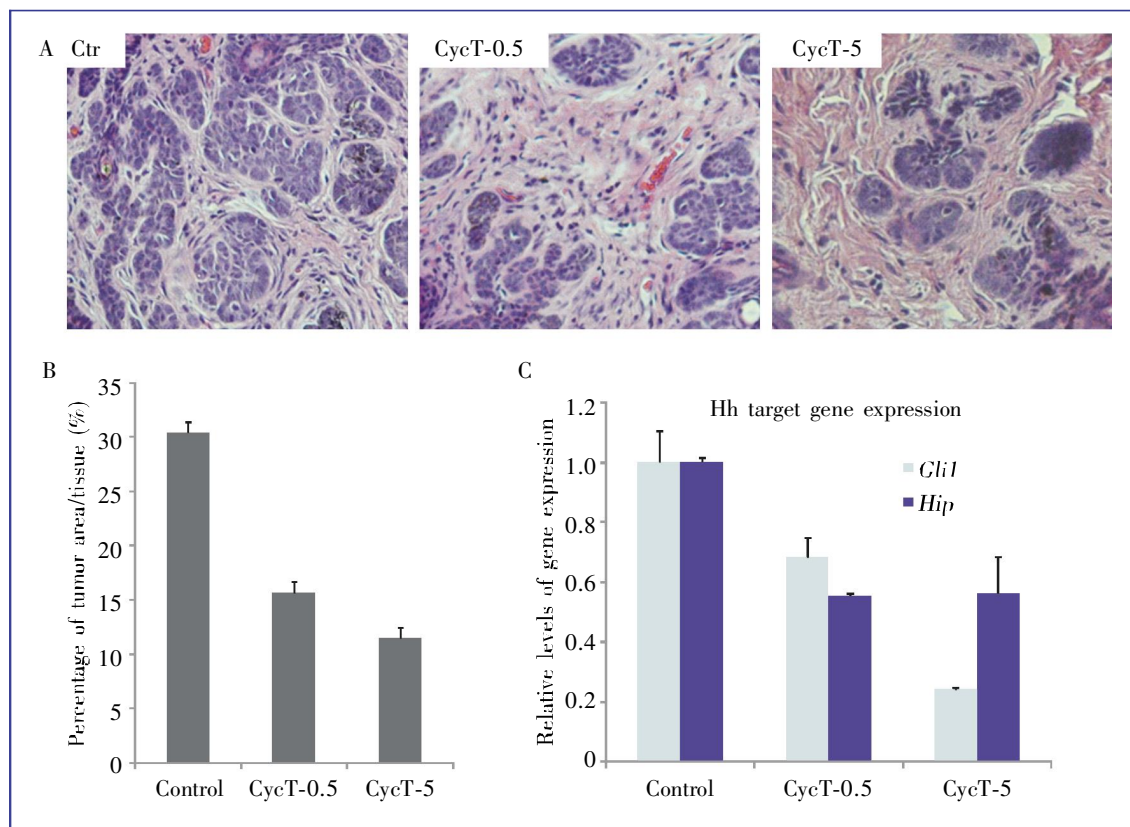


Figure 4. Effect of CycT on skin lesions from *Krt6a-cre:Ptch1^{neo/neo}* mice. Following drug treatment, mouse skin biopsies from the areas with drug administration were collected for HE staining. The effectiveness of CycT was examined by comparing the tumor areas between the two groups (A) and ImageJ analyses of 8 independent tissue areas per mouse (B, the average data from 6 mice in each group). While the skin in the control group contained ~30% of tumor area in the skin section, CycT-treated skin had only 10% to 15% of tumor area in the tissue. With 6 mice for each group, the statistical power for this study was 90.6. The level of Hh target gene expression was examined by real-time PCR (C), with both *Gli1* and *Hip* being down-regulated by CycT ($P < 0.05$ from unpaired Student's *t*-test for two samples).

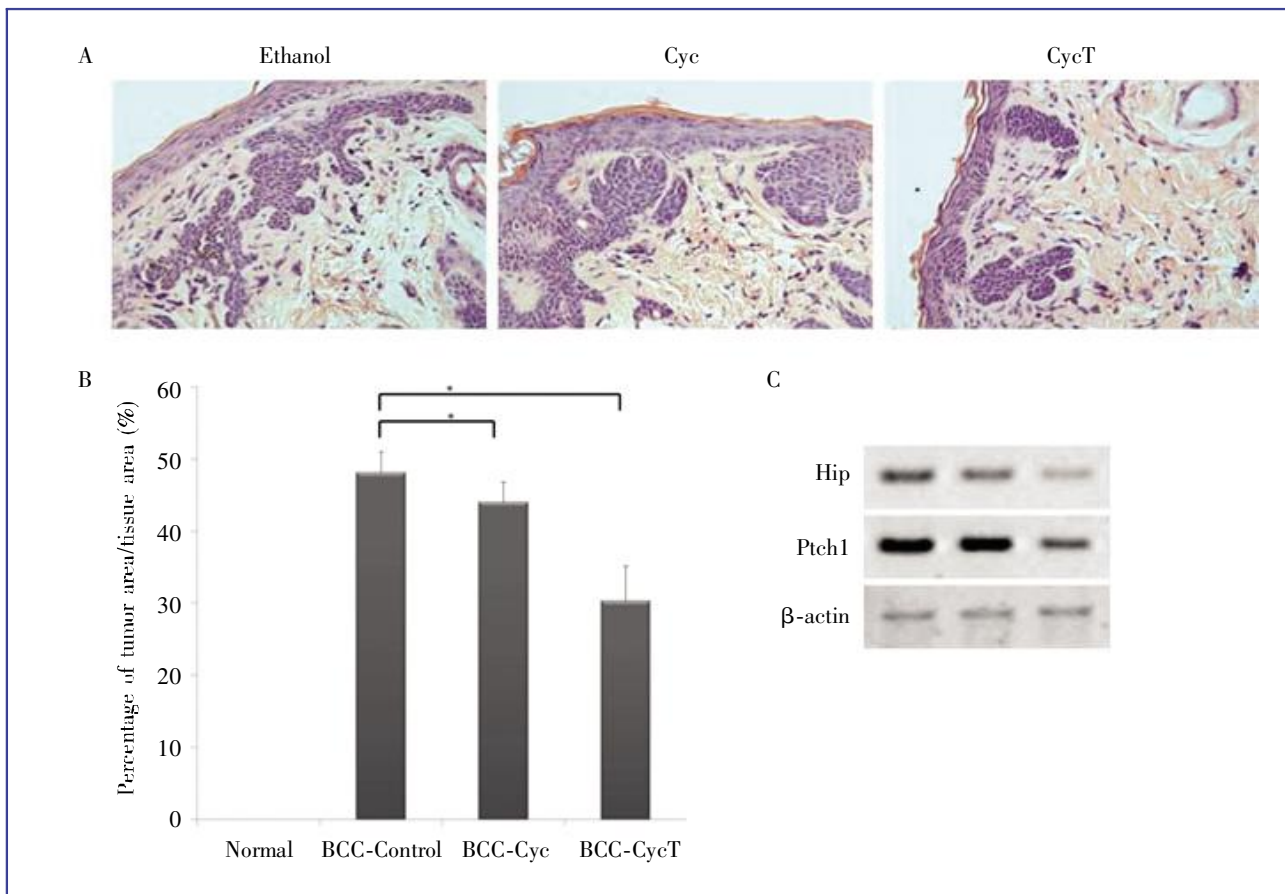


Figure 5. Comparing Cyc with CycT in tumor shrinkage of *Krt6a-cre:Ptch1^{neo/neo}* mice. A shows HE slides from different treatments. B shows the percentage of tumor area per tissue area in *Krt6a-cre:Ptch1^{neo/neo}* mice, which were generated from ImageJ analyses. * indicates significant differences between two samples ($P < 0.05$). We noticed that CycT-treated group had low tumor area value than Cyc-treated group. C shows RT-PCR data of hedgehog target genes and the β -actin control. CycT significantly reduced expression of HIP and Ptch1, whereas Cyc had little effects on hedgehog target gene expression.

specific inhibition of Hh signaling. These data further indicate that CycT is quite effective in inhibiting potent Hh signaling-induced carcinogenesis driven by loss of tumor suppressor *Ptch1* or expression of oncogenic Smo mutant *SmoM2*.

Discussion

Previous work has confirmed that Cyc is a valuable resource in the battle against BCCs and medulloblastomas^[23,26]. Despite the prominent potential of using Cyc as cancer therapeutic agent, several obstacles hamper its development and application, particularly its low solubility and weak potency for inhibiting Hh signaling. Therefore, efforts have been devoted into the synthesis of Cyc derivatives. In our studies, we observed significant variations in the plasma $T_{1/2}$ of both CycT and Cyc, which were different from a previous study in mice^[29] and sheep^[30]. Although CycT has some

improvements in water solubility and acute tolerance in mice, we think additional improvements are required for therapeutic use of CycT. At present, the solubility of CycT is still not very high (5–10 mg/mL), and it still has some toxicity in mice. Our studies in topical application of CycT on mouse BCCs suggest that bioavailability and bioactivity of CycT is reasonably high.

In this study, we examined the effects of Cyc and its tartrate salt (CycT) on Hh signaling-dependent motor neuron differentiation and Hh signaling-mediated carcinogenesis in mouse models. Following topical application of Cyc or CycT daily for 21 days, tumor shrinkage was observed in all mice, and these effects were associated with inhibition of Hh target genes. In all analyses, CycT was a more potent inhibitor of Hh signaling-mediated effects than Cyc. In the *Krt6a-cre:Ptch1^{neo/neo}* mouse model, the effect of CycT was comparable to the effect of KAAD-Cyc (data not shown), a Cyc derivative^[17]. Although KAAD-Cyc is not water soluble, its potency was significantly higher than Cyc

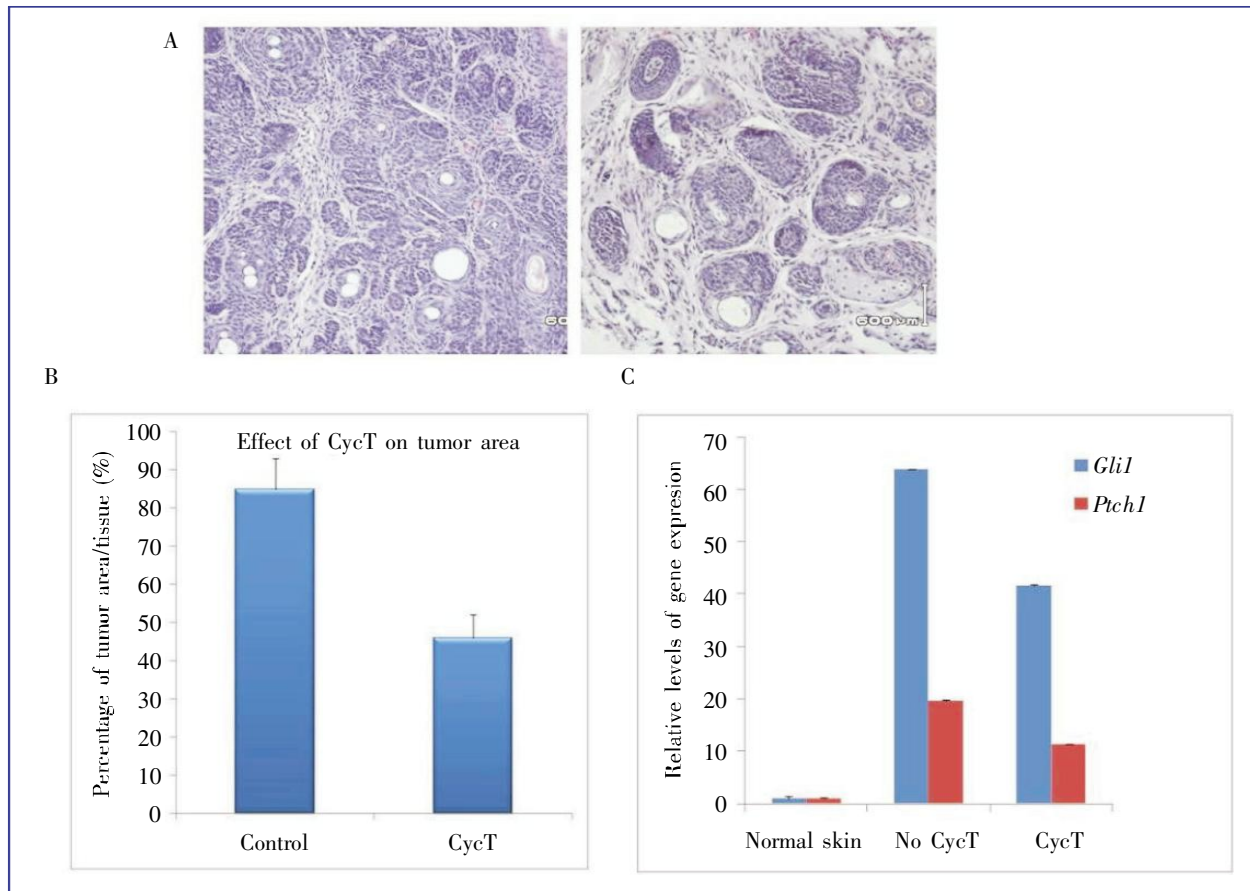


Figure 6. Effect of CycT on skin lesions from *Krt14-cre:SmoM2^{fl/fl}* mice. The effectiveness of CycT on SmoM2-mediated skin tumors was examined by comparing the tumor areas between the control and CycT-treated groups following drug treatment and HE staining (A) and imageJ analyses of 8 independent tissue areas (B). In this model, the percentage of tumor area in skin tissue was over 70% in the control group, but less than 40% in the CycT group. Each group had 10 mice, and the statistical power of this study was 100. The level of Hh target gene expression was examined by real-time PCR (C), with both *Gli1* and *Ptch1* down-regulated by CycT ($P < 0.05$ from unpaired Student's *t*-test for two samples).

[50% inhibition concentration (IC_{50}) = 20 nmol/L for KAAD-Cyc vs. 300 nmol/L for Cyc] (data not shown). Thus, as the known Hh signaling inhibitor KAAD-Cyc reduced tumor area by more than half in *Krt6a-cre:Ptch1^{neo/neo}* mice (data not shown), we concluded that our model is good for testing drugs with inhibitory effects on Hh signaling. The exact molecular basis for the high potency of CycT is currently unknown. We speculate that interaction of tartaric acid with Cyc may trap Cyc in a conformation more capable of efficient binding to SMO.

Due to low or undetectable Hh signaling activity in most cultured cells, there is a great need for a relatively simple and robust mouse model for *in vivo* assessment of the biological activities of Hh signaling inhibitors. In the present study, we used two mouse models of BCCs to assess the effect of CycT. One BCC mouse model is based on tissue-specific knockout of *Ptch1*, and the other is based on tissue-specific knock-in of activated *Smo*, *SmoM2¹²*. In both models, we detected skin lesions a few weeks after birth. Because they lacked fur, the mice

were amenable for topical application of compounds. Consistent with this phenotype, expression of Hh target genes in the epidermis of these mice was shown to be elevated. Topical application of drugs at relatively high concentrations (5 μ mol/L) had no significant effects on the survival or health of mice, suggesting little toxic effects of these compounds when applied topically. These data were substantiated by the effect of CycT on pancreatic cancer metastasis in an orthotopic mouse model (Figure 7). These *in vivo* mouse models provide useful tools to assess the effects of Cyc derivatives on Hh signaling-mediated carcinogenesis.

Hh signaling is activated in BCCs and medulloblastomas. The rationales to treat BCC and medulloblastomas with Hh signaling inhibitors are supported by both human cancer analyses and by animal models. However, the role of Hh signaling in other solid tumors is unclear. Our unpublished data indicate that Hh signaling is activated during pancreatic cancer metastasis (Figure 7). In an orthotopic mouse model of pancreatic

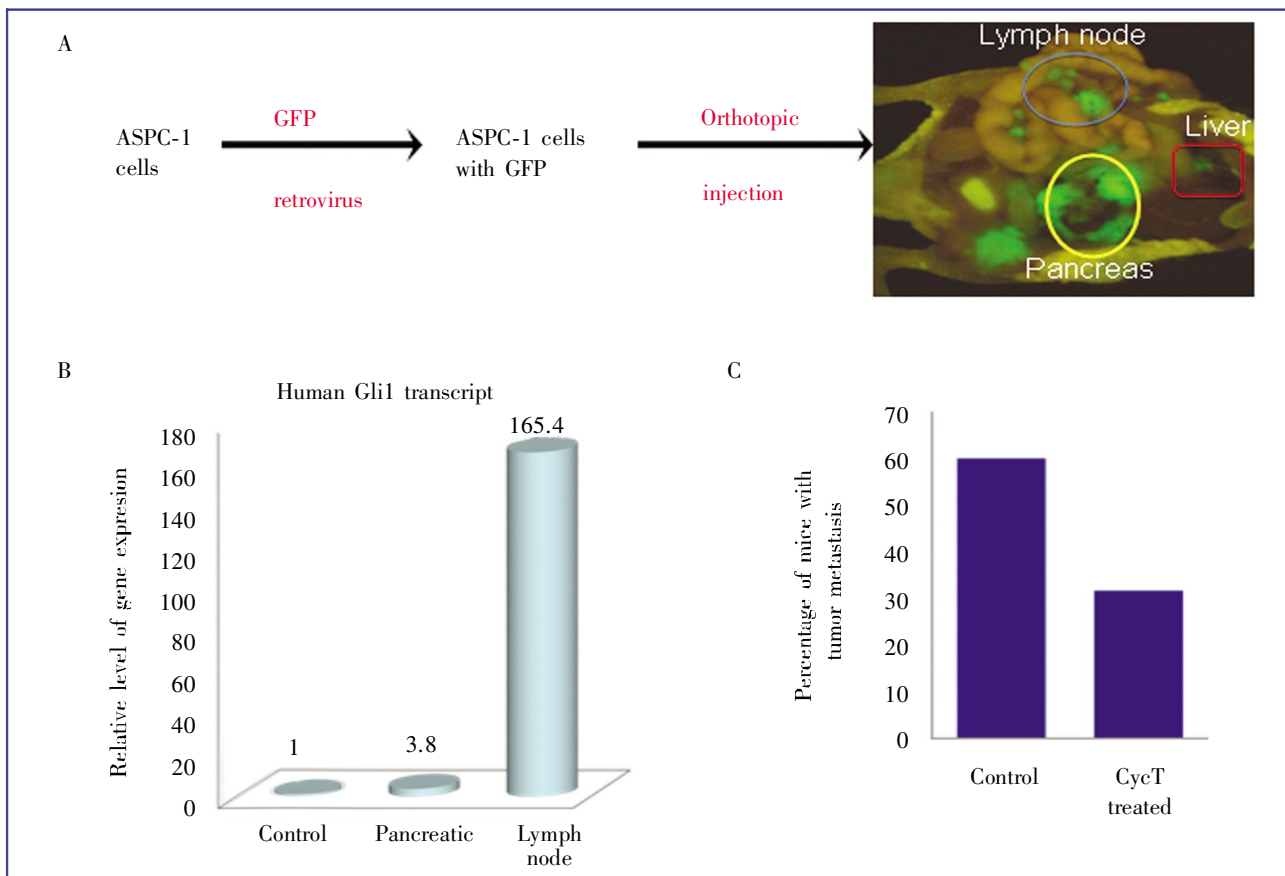


Figure 7. Effects of CycT on lymph node metastasis of pancreatic cancer. A shows the orthotopic model of pancreatic cancer metastasis. Mice were killed 6 weeks after GFP-expressing ASPC-1 cells were injected into the pancreas of NGS mice. GFP-positive tissues indicate tumor and its metastases in different organs (noticeably lymph nodes and liver). B shows expression of Hh target gene *Gli1*, indicating activation of hedgehog signaling pathway during pancreatic cancer metastasis. C shows the percentage of mice with lymph node metastases of tumor in two groups (control or CycT-treated), with 10 mice in each group.

cancer metastasis, our preliminary studies showed that 60% of mice in the control group had lymph node metastasis whereas only 30% of the mice in the CycT group had cancer metastasis (Figure 7), suggesting that CycT was effective in reducing lymph node metastasis of pancreatic cancer.

In summary, Cyc is insoluble in water, whereas CycT can be dissolved in water at 5 to 10 mg/mL. Our results show that the LD₅₀ of CycT (62.5 mg/kg body weight) is greater than that of Cyc (43.5 mg/kg body weight). In two independent mouse models of basal cell carcinomas, CycT induced tumor shrinkage, which was associated with decreased Hh target gene expression. These data

indicate that CycT is an effective Hh signaling inhibitor that warrants further investigation as a novel cancer therapeutic agent.

Acknowledgements

This research was supported by a grant from the National Institute of Health, USA (No. R01-CA94160).

Received: 2011-04-15; revised: 2011-04-20; accepted: 2011-04-25.

References

- [1] Nusslein-Volhard C, Wieschaus E. Mutations affecting segment number and polarity in drosophila [J]. *Nature*, 1980,287(5785): 795–801.
- [2] Bale AE. Hedgehog signaling and human disease [J]. *Annu Rev Genomics Hum Genet*, 2002,3:47–65.
- [3] Ingham PW, McMahon AP. Hedgehog signaling in animal

- development: paradigms and principles [J]. *Genes Dev*, 2001,15(23):3059–3087.
- [4] Yang L, Xie G, Fan Q, et al. Activation of the hedgehog-signaling pathway in human cancer and the clinical implications [J]. *Oncogene*, 2010,29(4):469–481.
- [5] Liu H, Gu D, Xie J. Clinical implications of hedgehog signaling pathway inhibitors [J]. *Chin J Cancer*, 2011,30(1):13–26.
- [6] Jiang J, Hui CC. Hedgehog signaling in development and cancer [J]. *Dev Cell*, 2008,15(6):801–812.
- [7] McMahon AP, Ingham PW, Tabin CJ. Developmental roles and clinical significance of hedgehog signaling [J]. *Curr Top Dev Biol*, 2003,53:1–114.
- [8] Sasaki H, Hui C, Nakafuku M, et al. A binding site for Gli proteins is essential for HNF-3beta floor plate enhancer activity in transgenics and can respond to Shh *in vitro* [J]. *Development*, 1997,124(7):1313–1322.
- [9] Kinzler KW, Ruppert JM, Bigner SH, et al. The GLI gene is a member of the kruppel family of zinc finger proteins [J]. *Nature*, 1988,332(6162):371–374.
- [10] Hahn H, Wicking C, Zaphiropoulos PG, et al. Mutations of the human homolog of *Drosophila* patched in the nevoid basal cell carcinoma syndrome [J]. *Cell*, 1996,85(6):841–851.
- [11] Johnson RL, Rothman AL, Xie J, et al. Human homolog of patched, a candidate gene for the basal cell nevus syndrome [J]. *Science*, 1996,272(5268):1668–1671.
- [12] Xie J, Murone M, Luoh SM, et al. Activating smoothened mutations in sporadic basaloid carcinoma [J]. *Nature*, 1998,391(6662):90–92.
- [13] Toftgard R. Hedgehog signalling in cancer [J]. *Cell Mol Life Sci*, 2000,57(12):1720–1731.
- [14] Pasca di Magliano M, Sekine S, Ermilov A, et al. Hedgehog/Ras interactions regulate early stages of pancreatic cancer [J]. *Genes Dev*, 2006,20(22):3161–3173.
- [15] Xie JW. Implications of hedgehog signaling antagonists for cancer therapy [J]. *Acta Biochimica Et Biophysica Sinica*, 2008,40(7):670–680.
- [16] Taipale J, Chen JK, Cooper MK, et al. Effects of oncogenic mutations in smoothened and patched can be reversed by cyclopamine [J]. *Nature*, 2000,406(6799):1005–1009.
- [17] Chen JK, Taipale J, Cooper MK, et al. Inhibition of hedgehog signaling by direct binding of cyclopamine to smoothened [J]. *Genes Dev*, 2002,16(21):2743–2748.
- [18] Jonkers J, Meuwissen R, van der Gulden H, et al. Synergistic tumor suppressor activity of BRCA2 and p53 in a conditional mouse model for breast cancer [J]. *Nat Genet*, 2001,29(4):418–425.
- [19] Mao J, Ligon KL, Rakhlin EY, et al. A novel somatic mouse model to survey tumorigenic potential applied to the hedgehog pathway [J]. *Cancer Res*, 2006,66(20):10171–10178.
- [20] Adolphe C, Hetherington R, Ellis T, et al. Patched1 functions as a gatekeeper by promoting cell cycle progression [J]. *Cancer Res*, 2006,66(4):2081–2088.
- [21] Keeler RF, Binns W. Teratogenic compounds of *Veratrum californicum* (Durand). V. Comparison of cyclopiian effects of steroidal alkaloids from the plant and structurally related compounds from other sources [J]. *Teratology*, 1968,1(1):5–10.
- [22] Sheng T, Chi S, Zhang X, et al. Regulation of Gli1 localization by the cAMP/protein kinase A signaling axis through a site near the nuclear localization signal [J]. *J Biol Chem*, 2006,281(1):9–12.
- [23] Athar M, Li C, Tang X, et al. Inhibition of smoothened signaling prevents ultraviolet B-induced basal cell carcinomas through regulation of Fas expression and apoptosis [J]. *Cancer Res*, 2004,64(20):7545–7552.
- [24] Wichterle H, Lieberam I, Porter JA, et al. Directed differentiation of embryonic stem cells into motor neurons [J]. *Cell*, 2002,110(3):385–397.
- [25] Mao J BJ, McMahon J, Vaughan J, et al. An ES cell system for rapid, spatial and temporal analysis of gene function *in vitro* and *in vivo* [J]. *Nucleic Acids Res*, 2005,33(18):e155.
- [26] Sinha S, Chen JK. Purmorphamine activates the hedgehog pathway by targeting smoothened [J]. *Nat Chem Biol*, 2006,2(1):29–30.
- [27] Fan Q, He M, Sheng T, et al. Requirement of TGFbeta signaling for SMO-mediated carcinogenesis [J]. *J Biol Chem*, 2010,285(47):36570–36576.
- [28] Berman DM, Karhadkar SS, Hallahan AR, et al. Medulloblastoma growth inhibition by hedgehog pathway blockade [J]. *Science*, 2002,297(5586):1559–1561.
- [29] Lipinski RJ, Hutson PR, Hannam PW, et al. Dose- and route-dependent teratogenicity, toxicity, and pharmacokinetic profiles of the hedgehog signaling antagonist cyclopamine in the mouse [J]. *Toxicol Sci*, 2008,104(1):189–197.
- [30] Welch KD, Panter KE, Lee ST, et al. Cyclopamine-induced synophthalmia in sheep: defining a critical window and toxicokinetic evaluation [J]. *J Appl Toxicol*, 2009,29(5):414–421.